DALTON

Mononuclear zinc(II), homodinuclear zinc(II) and heterodinuclear zinc(II)–copper(II) complexes derived from tris[(2-pyridyl)-methyl]amine

Harry Adams, Neil A. Bailey, David E. Fenton* and Qing-Yu He

Department of Chemistry, Dainton Building, The University of Sheffield, Sheffield S3 7HF7, UK

Mononuclear zinc(II), homodinuclear zinc(II) and heterodinuclear zinc(II)–copper(II) complexes derived from tris[(2-pyridyl)methyl]amine (L) have been prepared and characterised. The crystal structures of two mononuclear complexes, $[ZnL(Cl)][BPh_4]\cdot MeCN$ and $[ZnL(O_2CPh)][BPh_4]$ show that the co-ordination geometries around the zinc are close to trigonal bipyramidal and that of the heterodinuclear complex $[ZnCuL_2(p\text{-}O_2NC_6H_4OPO_3)][BPh_4]_2\cdot H_2O$ shows that the metal atoms are separated by 5.86 Å and bridged by a phosphate monoester.

A number of zinc enzymes, alkaline phosphatase,[1] leucine aminopeptidase,[2] P1 nuclease,[3] phospholipase C,[4] phosphotriesterase,[5] and *Aeromonas proteolytica* aminopeptidase,[6] containing two, or more, zinc atoms in co-catalytic, or coactive, sites has been identified and structurally characterised and comprehensively reviewed.[7–11] As a result investigations have begun into the use of multinuclear zinc complexes as biomimetic compounds.[12–17]

Water is the ubiquitous ligand at the catalytic zinc site in zinc enzymes.[18,19] One pathway for reactivity is the generation of a Zn–OH moiety, through enhancement of the acidity of the co-ordinated water by the superacidic zinc, to provide nucleophiles for the hydrolysis of carboxylic and phosphate esters,[20–22] the hydrolysis of peptidic amides[23] and the hydration of CO_2.[24] Studies in aqueous solution have shown that $[ZnL(H_2O)]^{2+}$, where L is the tetradentate ligand tris[(2-pyridyl)methyl]amine, can form the corresponding $[ML(OH)]^+$ species at relatively low pH values[25] and Murthy and Karlin[12] have recently shown that the dinuclear zinc complex $[LZn(\mu\text{-}OH)_2ZnL][ClO_4]_2$ can trap atmospheric CO_2 to give the trinuclear complex $[\{ZnL\}_3(\mu_3\text{-}CO_3)][ClO_4]_4\cdot H_2O$.

The polypodal co-ordinating properties of L indicate that it can form five-co-ordinate zinc complexes with additional ligation from an exogenous anionic or neutral (*e.g.* H_2O) ligand through which multinuclear zinc complexes can be constructed and to that end we have demonstrated that the dicationic complex $[LZn(\mu\text{-}OH)_2ZnL]^{2+}$ reacts with mono(*p*-nitrophenyl) phosphate to give the dinuclear complex $[LZn(p\text{-}O_2NC_6H_4OPO_3)ZnL][BPh_4]_2$. The Zn · · · Zn separation in this complex is 5.97 Å and the phosphate bridges in a *syn-anti* mode.[26] This distance however is well in excess of the value of 3.94 Å found in the crystal structure of the zinc pair present in the *Escherichia coli* alkaline phosphatase–inorganic phosphate complex,[1] illustrating the difficulty of reproducing features of a metallobiosite through the use of small-molecule models in which the steric controls implicit in the protein structure are absent.

In the current work we show that the carboxylate anion is not effective in supporting a bridge between two $[ZnL]^{2+}$ moieties, and report the crystal structure of the heterodinuclear (Zn,Cu) analogue of $[LZn(p\text{-}O_2NC_6H_4OPO_3)ZnL][BPh_4]_2$.

Experimental

Elemental analyses were carried out by the University of Sheffield Microanalytical Service. Infrared spectra were recorded as KBr discs using a Perkin-Elmer 1710 Fourier-transform spectrophotometer (4000–400 cm^{-1}), ^1H NMR spectra at 220 MHz on a Perkin-Elmer R34 spectrometer and positive-ion fast atom bombardment (FAB) mass spectra on a Kratos Ms 80 spectrometer using a 3-nitrobenzyl alcohol matrix unless otherwise stated.

CAUTION: although no problems were encountered during the use of perchlorate salts as described below, suitable care and precautions should be taken when handling such potentially hazardous compounds.

Tris[(2-pyridyl)methyl]amine (L) was prepared using the literature procedure.[27]

Preparations

$[Zn_2L_2(\mu\text{-}OH)_2][BF_4]_2$ 1. This complex was prepared from $Zn(BF_4)_2\cdot H_2O$ (1 mmol, 0.24 g) by adoption of the literature procedure[12] for $[Zn_2L_2(\mu\text{-}OH)_2][ClO_4]_2$. Yield = 0.35 g, 68%. IR(KBr disc, $\tilde{\nu}/cm^{-1}$): 3640 (OH), 1609 (C=N of py), 1480, 1434, 1155, 1054. Positive-ion FAB mass spectrum: *m/z* = 453 {$ZnL(BF_4)$], 24}, 389 {[$ZnL(OH)_2$], 100} and 372 {[ZnL(OH)], 15%) [Found ($C_{36}H_{38}B_2F_8N_8O_2Zn_2$ requires): C, 47.0 (47.15); H, 4.3 (4.2); N, 12.4 (12.25)%].

$[ZnL(Cl)][BPh_4]\cdot MeCN$ 2. Sodium chloride (1 mmol, 0.06 g) in MeOH (10 cm^3) was added to a methanolic solution containing equimolar amounts of L (0.29 g) and $Zn(BF_4)_2\cdot H_2O$ (0.24 g). The mixture was heated to reflux for 1 h. Sodium tetraphenylborate (1 mmol, 0.32 g) in MeOH (5 cm^3) was added dropwise to the clear solution and some white precipitate emerged. After stirring at reflux temperature for 1 h and cooling, the resulting white powder was filtered off. Recrystallisation of the powder from MeCN–MeOH (1:3) generated clear square crystals suitable for X-ray crystallography. Yield = 0.52 g, 75%. IR(KBr disc, $\tilde{\nu}/cm^{-1}$): 1608 (C=N of py), 736 and 709 (Ph_4B). Positive-ion FAB mass spectrum: *m/z* = 389 {[ZnL(Cl)], 100%} [Found ($C_{44}H_{41}BClN_5Zn$ requires): C, 69.65 (70.3); H, 5.6 (5.5); Cl, 4.9 (4.7); N, 9.15 (9.3)%].

$[ZnL(O_2CPh)][BPh_4]\cdot 2H_2O$ 3. To a clear methanolic solution containing L (1 mmol) was added an equimolar amount of $Na(O_2CPh)$ (0.15 g) in MeOH (5 cm^3). The solution was adjusted to pH ≈ 8.5 by addition of NEt_3 and heated to reflux for 2 h. On cooling the solvent was evaporated to near dryness. Methanol–ethyl acetate (1:5, 40 cm^3) was added to dissolve the residue and $NaBPh_4$ (1 mmol, 0.33 g) in MeOH (5 cm^3) was added dropwise. A yellow-white precipitate emerged immediately and the suspension was stirred at room temperature for 2 h before filtering to collect the crystalline solid. Recrystallisation of the solid from hot MeOH gave light yellow crystals suitable

for X-ray crystallography. Yield = 0.56 g, 82%. IR(KBr disc, $\tilde{\nu}/cm^{-1}$): 1610 (C=N of py), 1575, 1564 and 1364 (RCO_2), 733 and 706 (Ph_4B), 612. Positive-ion FAB mass spectrum: *m/z* = 475 {[ZnL(O_2CPh)], 100%}[2] [Found (bulk sample) ($C_{49}H_{47}BN_4O_4Zn$ requires): C, 70.6 (70.7); H, 5.8 (5.7); N, 6.35 (6.7)%].

[ZnL(O_2CMe)][BPh_4] 4. This was prepared from L (1 mmol, 0.29 g) and $Zn(O_2CMe)_2$ (1 mmol, 0.19 g) in MeOH at pH ≈ 8.5 (3 mol dm^{-3} NaOH) by a similar procedure to that described above. After treatment with $NaBPh_4$ at reflux temperature for 1 h, the resulting yellow-white crystalline powder was filtered off and recrystallised from MeCN–MeOH (1:5). Yield = 0.53 g, 80%. IR(KBr disc, $\tilde{\nu}/cm^{-1}$): 1609 (C=N of py), 1577 and 1382 (RCO_2), 735 and 706 (Ph_4B). Positive-ion FAB mass spectrum: *m/z* = 413 {[ZnL(O_2CMe)], 100%} [Found ($C_{44}H_{41}BN_4O_2Zn$ requires): C, 71.25 (71.0); H, 5.45 (5.6); N, 7.6 (7.6)%].

[Zn_2L_2(*p*-$O_2NC_6H_4OPO_3$)][BPh_4]$_2$·2H_2O 5. A methanolic solution (50 cm^3) of L (1 mmol, 0.29 g) and $Zn(BF_4)_2·H_2O$ (1 mmol, 0.24 g) at pH ≈ 8.5 (3 mol dm^{-3} NaOH) was stirred with refluxing for 30 min to form a clear solution of complex **1**. Mono-*p*-nitrophenyl phosphate (0.5 equivalent) in MeOH (15 cm^3) was added dropwise to the above warm solution,which was then refluxed for 1 h. Sodium tetraphenylborate (1 mmol, 0.33 g) in MeOH (5 cm^3) was added and the mixture was stirred for another hour. After cooling, the suspension was filtered to collect yellow-white microcrystals. The product was recrystallised from MeCN–MeOH (1:2) as single crystals. Yield = 0.52 g, 51%. NMR (CD_3CN): ^{1}H, δ 4.05 (s, 12 H, CH_2), 6.85 (t, 6 H, H^5 of py), 6.95–7.30 (m, 40 H, PhB), 7.45 (d, 6 H, H^3 of py), 7.60 (d, 2 H, $C^{2,6}H$ of C_6H_4), 7.90 (t, 6 H, H^4 of py), 8.15 (d, 2 H, $C^{3,5}H$ of C_6H_4) and 9.25 (d, 6 H, H^6 of py); ^{31}P, δ −0.62. IR(KBr disc, $\tilde{\nu}/cm^{-1}$): 1609 (C=N of py), 1339 (NO), 1267 and 1146 (PO), 734 and 707 (Ph_4B). Positive-ion FAB mass spectrum: (X = $O_2NC_6H_4OPO_3$): *m/z* = 1250 {[$L_2Zn_2L_2$(X)(BPh_4)], 15} 928 {[Zn_2L_2X], 14} and 572 {[ZnL(X)], 48%} [Found ($C_{90}H_{84}B_2N_9O_8PZn_2$ requires): C, 67.2 (67.4); H, 5.4 (5.3); N, 8.05 (7.9)%].

[Zn_2L_2(*p*-$O_2NC_6H_4OPO_3$)][ClO_4]$_2$·3H_2O 6. This was prepared from $Zn(ClO_4)_2·6H_2O$ with the same procedure as for complex **5.** The resulting mixture was filtered and the clear filtrate allowed to stand at room temperature overnight. White needle crystals were deposited. Yield = 0.51 g, 56%. 1H NMR (CD_3CN): δ 4.30 (s, 12 H, CH_2), 6.92 (t, 6 H, H^5 of py), 7.60 (d, 6 H, H^3 of py), 7.70 (d, 2 H, $C^{2,6}H$ of C_6H_4), 7.93 (t, 6 H, H^4 of py), 8.20 (d, 2 H, $C^{3,5}H$ of C_6H_4), 8.90 (d, 6 H, H^6 of py). IR(KBr disc, $\tilde{\nu}/cm^{-1}$): 1612 (C=N of py), 1254 and 1155 (PO), 1095 and 623 (ClO_4). Positive-ion FAB mass spectrum: *m/z* = 1028 {[$Zn_2L_2X(ClO_4)$], 25} and 572 {[ZnL(X)], 24%} [Found ($C_{42}H_{46}Cl_2N_9O_{17}PZn_2$ requires): C, 42.7 (42.7); H, 3.65 (3.9); N, 10.85 (10.7)%].

[Zn_2L_2($HOPO_3$)][BPh_4]$_2$·H_2O 7. This was prepared from Na_2HPO_4 (0.5 mmol) in water (3 cm^3) by following a similar procedure to that for complex **5**. Recrystallisation of the resulting crystalline powder from MeCN–MeOH (3:1) gave clear crystals that readily lost solvent on exposure to the atmosphere. The microanalysis data listed below are those for a dried sample. Yield = 0.39 g, 44%. NMR (CD_3CN): ^{1}H, δ 4.05 (s, 12 H, CH_2), 6.80 (t, 6 H, H^5 of py), 6.90–7.30 (m, 40 H, PhB), 7.45 (d, 6 H, H^3 of py), 7.75 (t, 6 H, H^4 of py) and 9.10 (d, 6 H, H^6 of py); ^{31}P, δ 2.21. IR(KBr, $\tilde{\nu}/cm^{-1}$): 3422 (OH), 1609 (C=N of py), 1269 and 1127 (PO), 733 and 705 (Ph_4B). Positive-ion FAB mass spectrum (X = HPO_4): *m/z* = 1127 {[$Zn_2L_2X(BPh_4)$], 9}, 807 {[Zn_2L_2(X)], 15} and 451 {[ZnL(X)], 16%} [Found ($C_{84}H_{77}B_2N_8O_4PZn_2$ requires): C, 69.7 (69.8); H, 5.7 (5.4); N, 7.7 (7.75)%].

[$ZnCuL_2$(*p*-$O_2NC_6H_4OPO_3$)][BPh_4]$_2$·H_2O 8. This was prepared by following a similar procedure to that for complex **5** with equimolar amounts (0.5 mmol) of $Zn(BF_4)_2·H_2O$ and $Cu(BF_4)_2·H_2O$ being added to the solution. The green crystalline product was recrystallised from MeCN–MeOH (3:1) to give light green needle crystals of complex **8**. Yield = 0.63 g, 60%. IR(KBr disc, $\tilde{\nu}/cm^{-1}$): 1608 (C=N of py), 1342 (NO_2), 1262 and 1128 (PO), 734 and 707 (Ph_4B). Positive-ion FAB mass spectrum: (X = $O_2NC_6H_4OPO_3$): *m/z* = 1246 {[$ZnCuL_2X$-(BPh_4)], 13}, 926 {[$ZnCuL_2X$], 37}, 355 (ZnL, 46) and 353 (CuL, 100%); accurate mass: 924.142 021($ZnCuL_2X$ requires 924.142 664). Microanalysis for bulk sample [Found tetrahydrate $C_{90}H_{88}B_2CuN_9O_{10}PZn$ requires): C, 66.15 (66.1); H, 5.45 (5.4); N, 7.5 (7.7)%].

Crystallography

Crystal data and experimental conditions for complexes **2**, **3** and **8**, are listed in Table 1.

Complex 2. Three-dimensional, room-temperature X-ray data were collected in the range 3.5 < 2θ < 45° on a Siemens P4 diffractometer by the ω-scan method. Of the 6168 reflections measured, all of which were corrected for Lorentz-polarisation effects (but not for absorption), 3852 independent reflections exceeded the significance level $|F|/\sigma(|F|) > 4.0$. The structure was solved by direct methods and refined by full-matrix least-squares methods on F^2. Hydrogen atoms were included in calculated positions and refined in riding mode. Refinement converged to a final $R = 0.0480$ ($wR2 = 0.1326$ for all 5011 reflections, 454 parameters, mean and maximum δ/σ 0.00, 0.06), with allowance for the thermal anisotropy of all non-hydrogen atoms. Minimum and maximum final electron density 0.376 and −0.572 e $Å^{-3}$. A weighting scheme $w = 1/[\sigma^2(F_o^2) + (0.0713P)^2 + 1.76P]$ where $P = (F_o^2 + 2F_c^2)/3$ was used in the latter stages of refinement.

Complex 3. Data were collected as above. Of the 9514 reflections measured, all of which were corrected for Lorentz-polarisation effects (but not for absorption), 4448 independent reflections exceeded the significance level $|F|/\sigma(|F|) > 4.0$. The structure was solved and refined as above to a final $R = 0.0957$ ($wR2 = 0.3484$, for all 8178 reflections, 514 parameters, mean and maximum δ/σ 0.000, 0.010), with allowance for the thermal anisotropy of all non-hydrogen atoms. Minimum and maximum final electron density −0.691 and 1.346 e $Å^{-3}$. A weighting scheme $w = 1/[\sigma^2(F_o^2) + (0.2031P)^2 + 20.9112P]$ where $P = (F_o^2 + 2F_c^2)/3$ was used in the latter stages of refinement.

Complex 8. Three-dimensional, room-temperature X-ray data were collected in the range 3.5 < 2θ < 50° on a Enraf-Nonius FAST TV area detector. Of the 37 216 reflections measured, all of which were corrected for Lorentz-polarisation effects (but not for absorption), 2316 independent reflections exceeded the significance level $|F|/\sigma(|F|) > 4.0$. The structure was solved and refined as above. The metal atom sites were assumed 50:50 disordered Cu:Zn (in the absence of clear geometric distinction), and were so refined with Zn(1) and Cu(1a) coincident, as were Cu(1) and Zn(1a). The six-membered ring of the *p*-nitrophenyl was refined with constrained *D*6*l* geometry. Refinement converged to a final $R = 0.0811$ ($wR2 = 0.2150$, for all 12 920 data, 513 parameters, mean and maximum δ/σ 0.000, 0.000), with allowance for the thermal anisotropy of only metals, phosphorus, oxygen and nitrogen atoms (excluding those of the nitro group). Minimum and maximum final electron density −0.391 and 0.841 e $Å^{-3}$. A weighting scheme $w = 1/[\sigma^2(F_o^2) + (0.0718P)^2 + 0.000P]$ where $P = (F_o^2 + 2F_c^2)/3$ was used in the latter stages of refinement.

For all structures complex scattering factors were taken from the program package SHELXL 93[28] as implemented on a Viglen 486dx computer.

Table 1 Crystal data and structure refinement for $[ZnL(Cl)][BPh_4]\cdot MeCN$, $[ZnL(O_2CPh)][BPh_4]$ and $[ZnCuL_2(p\text{-}O_2NC_6H_4OPO_3)][BPh_4]_2\cdot H_2O$ *

Empirical formula	$C_{44}H_{41}BClN_5Zn$	$C_{49}H_{43}BN_4O_2Zn$	$C_{90}H_{82}B_2CuN_9O_7PZn$
M	751.45	796.05	1583.15
Space group	$P2_1/c$	$C2/c$	$P2_1/c$
a/Å	14.270(4)	32.276(10)	17.904(7)
b/Å	18.012(5)	12.74(2)	33.436(5)
c/Å	15.152(4)	23.82(2)	14.783(3)
β/°	100.84(3)	108.54(4)	110.52(3)
U/Å^3	3825(2)	9286(7)	8288(4)
Z	4	8	4
D_c/Mg m^{-3}	1.305	1.139	1.269
μ/mm^{-1}	0.750	0.569	0.625
F(000)	1568	3328	3300
Crystal size/mm	0.75 × 0.41 × 0.20	0.55 × 0.35 × 0.25	0.65 × 0.22 × 0.22
θ Range for data collection/°	1.78–22.52	1.80–24.99	1.91–25.07
hkl Ranges	−1 to 15, −1 to 19, −16 to 16	−1 to 38, −1 to 15, −28 to 27	−21 to 20, −37 to 38, −16 to 12
Reflections collected	6168	9514	37 216
Independent reflections (R_{int})	5011 (0.0262)	8178 (0.0293)	12 920 (0.2265)
Data, restraints, parameters	5011, 0, 454	8177, 0, 514	12 920, 11, 513
Goodness of fit on F^2	1.034	1.013	0.600
Final *R*1, *wR*2 indices [$I > \sigma(I)$]	0.0480, 0.1188	0.0957, 0.2801	0.0811, 0.1721
(all data)	0.0689, 0.1326	0.1572, 0.3484	0.2732, 0.2150
Largest difference peak and hole/e Å^{-3}	0.376, −0.572	1346, −0.691	0.841, 0.391

* Details in common: 293(2) K; Mo-Kα radiation (λ 0.710 73 Å); monoclinic.

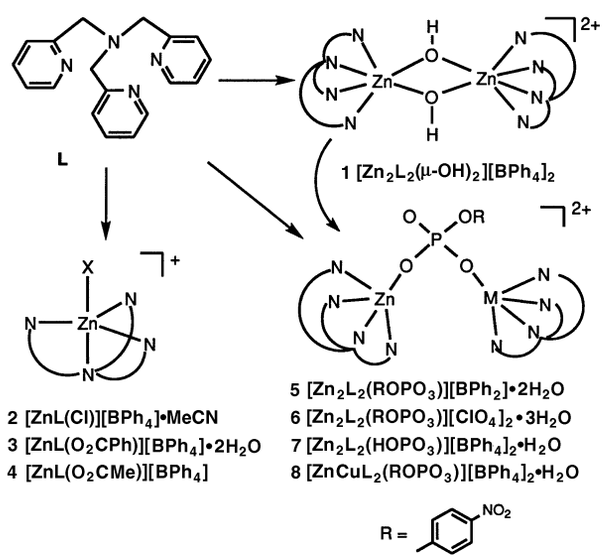

Scheme 1 Synthesis of Zn, Zn–Zn and Zn–Cu complexes of tris-[(2-pyridyl)methyl]amine (L)

Atomic coordinates, thermal parameters, and bond lengths and angles have been deposited at the Cambridge Crystallographic Data Centre (CCDC). See Instructions for Authors, *J. Chem. Soc.*, *Dalton Trans*, 1997, Issue 1. Any request to the CCDC for this material should quote the full literature citation and the reference number 186/460.

Results and Discussion

The synthesis of zinc complexes of L is illustrated in Scheme 1. Complex **1** was prepared according to the literature procedure for the analogous perchlorate complex. In this complex the zinc ion is in a distorted octahedral co-ordination environment with ligation by four ligand N atoms and two bridging hydroxide O atoms; the zinc–zinc separation is 2.992 Å.[12]

Addition of NaCl to a solution containing L and $Zn(BF_4)_2$, followed by treatment with $NaBPh_4$, gave complex **2** as a crystalline white powder. Recrystallisation from MeCN–MeOH produced light straw-coloured crystals suitable for X-ray crystallography. The FAB mass spectrum of the product gave a set peaks with the isotopic pattern for the parent fragment $[ZnL(Cl)]^+$ at 389 (100), 390 (22), 391 (92) and 392 (28%) confirming the presence of Cl^- as a coligand. The elemental analysis of the complex suggested the presence of a molecule of MeCN.

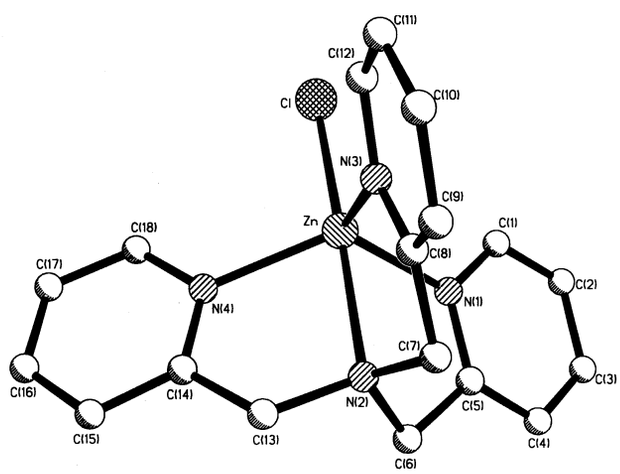

Fig. 1 Molecular structure of the cation $[ZnL(Cl)]^+$

The crystal structure of complex **2** reveals that each complex molecule consists of a mononuclear zinc unit, a solvent MeCN molecule and a tetraphenylborate anion. The molecular structure of the complex cation is illustrated in Fig. 1 and selected bond lengths and angles are given in Table 2. The co-ordination geometry at the zinc atom is very close to trigonal bipyramidal; three equivalent pyridine N atoms constitute the trigonal plane with Zn–N bond lengths in the range 2.063–2.080 Å and N–Zn–N bond angles in the range 109.95–121.88°. The zinc atom lies above this plane in the direction of chloride and the root-mean-square deviation from the plane is 0.204 Å. The chloride ion and the bridgehead N atom are axially bound to the zinc with almost equivalent bond lengths [Zn–Cl 2.2754 and Zn–N(2) 2.271 Å] and are almost linearly aligned with the zinc atom [Cl–Zn–N(2) 177.90°].

The co-ordination geometry of zinc in complex **2** is very similar to that found for zinc(II) in the complex $[ZnL(Cl)][ClO_4]$[29] and is also similar to that found for the complex cation $[ZnL^1(Cl)]^+$ where L^1 is the closely related tripodal ligand tris(*N*-methylbenzimidazolyl-2-methyl)amine.[30] In this cation

Table 2 Selected bond lengths (Å) and angles (°) for [ZnL(Cl)]-[BPh_4]·MeCN

Zn–N(1)	2.064(3)				
Zn–N(2)	2.271(3)	77.41(12)			
Zn–N(3)	2.063(3)	115.20(14)	78.10(13)		
Zn–N(4)	2.080(3)	121.88(14)	78.14(12)	109.95(13)	
Zn–Cl	2.2754(14)	102.26(10)	177.90(9)	103.90(11)	100.46(10)
		N(1)	N(2)	N(3)	N(4)

Table 3 Selected bond lengths (Å) and angles (°) for [ZnL(O_2CPh)]-[BPh_4]

Zn–N(1)	2.067(6)				
Zn–N(2)	2.262(6)	76.2(2)			
Zn–N(3)	2.060(6)	112.6(3)	77.4(2)		
Zn–N(4)	2.066(7)	119.6(3)	78.3(2)	113.9(3)	
Zn–O(1)	1.953(7)	104.3(3)	173.4(3)	96.4(3)	106.5(3)
		N(1)	N(2)	N(3)	N(4)

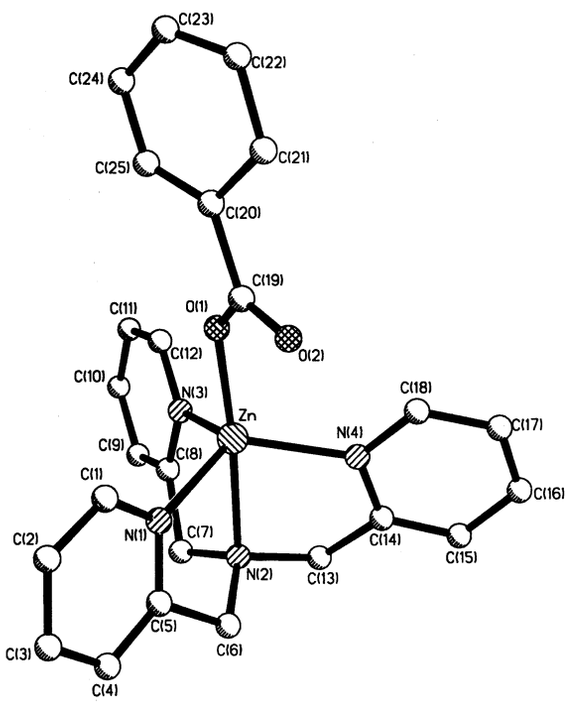

Fig. 2 Molecular structure of the cation [ZnL(O_2CPh)]$^+$

the chloride and bridgehead N atoms are axial with bond distances of 2.252 (Zn–Cl) and 2.480 Å (Zn–N) and the Cl–Zn–N angle is 178.6°. All three structures reveal the presence of a large axial opening for an exogenous coligand. The addition of a potential bidentate coligand capable of linking two metal centres through the axial position can lead to the formation of a dinuclear complex. A dinuclear complex of L having a carbonate bridge, [LCu(μ-CO_3)CuL]$^{2+}$ has been reported[31] as has a related dizinc complex derived from a relatively rigid tripodal tris(3-*tert*-butyl-5-methylpyrazolyl)hydroborate ligand, [$Zn_2L^2{}_3$][CO_3].[32]

After addition of sodium benzoate to a methanolic solution of complex **1**, under N_2 at pH ≈ 8.5, the solution was treated with $NaPh_4$; the resulting solid was recrystallised from methanol–ethyl acetate to give light yellow crystals of complex **3**. When the complexation reaction was carried out using L and zinc acetate, at pH ≈ 8.5, followed by treatment with $NaPh_4$, complex **4** was obtained as a microcrystalline powder. The IR spectra of both complexes exhibit symmetric and asymmetric stretches of the carboxylates confirming the presence of benzoate and acetate. The FAB mass spectra display parent peaks at *m/z* = 475 for **3** and 413 for **4**, corresponding to the mono-

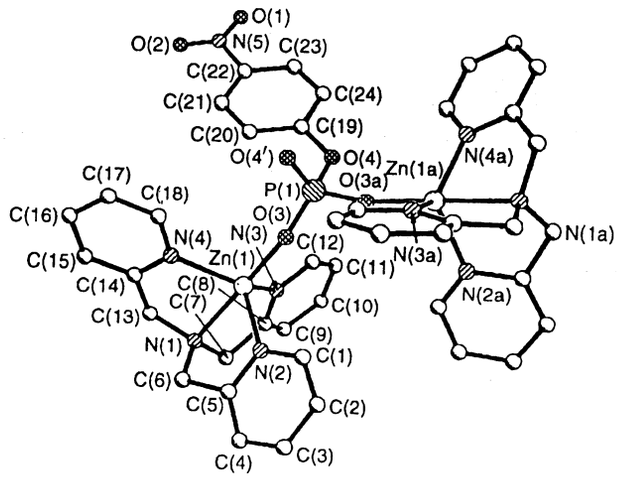

Fig. 3 Molecular structure of the cation [LZn(*p*-$O_2NC_6H_4OPO_3$)-ZnL]$^{2+}$

nuclear fragments [ZnL(X)] (X = carboxylate); no signals were found that could be assigned to carboxylate-bridged dinuclear species [Zn_2L_2X].

The crystal structure of complex **3** confirmed that it is a mononuclear zinc species (Fig. 2) comprised of a complex zinc cation and a [BPh_4]$^-$ counter anion; selected bonds and angles are given in Table 3. As in **2**, the co-ordination geometry at the zinc atom is close to trigonal bipyramidal. Three pyridine N atoms are equatorially co-ordinated to the zinc which lies 0.195 Å above the triangle plane in the direction of the axial benzoate O atom. The dihedral angles between pyridine rings are 118.2, 118.1 and 123.4° respectively. The tertiary amine N atom is axially bound to the zinc at 2.262 Å and the benzoate group occupies the open axial position in a monodentate mode and with a Zn–O(1) distance of 1.953 Å. The angle O(1)–Zn–N(2) is 173.4°, smaller than the axial angle 177.9° in **2**. This is possibly due to the presence of the benzoate 'keto' oxygen which is sited in the space between two of pyridine rings causing the large dihedral angle (123.4°) between the two pyridine planes. The structure of a salicylate-containing complex derived from tris-(benzimidazolyl-2-methyl)amine (L^3), [ZnL^3(sal)][ClO_4], shows a similar trigonal-bipyramidal geometry at the metal.[33] The salicylate binds in a monodentate mode through the carboxylate and the Zn–O distance is 1.961 Å; the Zn–N (bridgehead) distance is much longer at 2.515 Å. In the corresponding complex with benzoate as the coligand, [ZnL^2(O_2CPh)][BF_4], the overall structural features are very similar; the Zn–O distance is 1.988 Å and the Zn–N (bridgehead) distance is 2.520 Å.[34] The metal atom is clearly pulled closer in to the bridgehead N atom in the pyridinyl-based ligand than it is in the benzimidazolyl-based ligands; this may reflect a stronger donor capability in the former ligand.

The above experiments showed that the carboxylate groups did not link two ZnL units to form dinuclear complexes. Therefore the use of a phosphate bridging group in building dinuclear species was explored. A methanolic solution containing mono(*p*-nitrophenyl) phosphate was added to a solution of **1** and the mixture was treated, whilst hot, with $NaBPh_4$. Complex **5** was recovered as a solid which was recrystallised to give crystals suitable for structure determination. An analogous complex, **6**, was prepared as microcrystals, starting from zinc perchlorate instead of zinc tetrafluoroborate.

A preliminary report of the structure of complex **5** shows that there are two dinuclear zinc units in the complex linked by co-ordination of the phosphate as a bridging group.[26] The structure of the cation is illustrated in Fig. 3. Four N atoms from each ligand L co-ordinate to each zinc atom, and the phosphate bridges the two complex units such that each zinc atom adopts a trigonal-bipyramidal geometry. The zinc–zinc separation is 5.97 Å and this may be compared with the dis-

tance of 5.14 Å found in the related neutral dizinc complex [L^4Zn{OP(O)($OC_6H_4NO_2$)O}ZnL^4] [L^4 = tris(3,5-diisopropylpyrazol-1-yl)hydroborate].[14] In both of these complexes the interzinc distance is well in excess of the value of 3.94 Å found for the zinc pair in alkaline phosphatase. In the latter the co-ordination mode of the phosphate is *syn-syn* whereas in the synthetic analogues the phosphate bridges in a *syn-anti* mode. Furthermore in the small-molecule models the metal environments are not subject to any constraints that might be imposed by the presetting of a metal-binding cleft by the protein.

Absorption bands occurring at ≈1260 and ≈1150 cm^{-1} in the IR spectra of the two phosphate-bridged dinuclear complexes **5** and **6** can be assigned to co-ordinated phosphate P–O stretches.[35] The FAB mass spectra of both complexes display mononuclear parent fragments [ZnL(X)] (X = phosphate) at *m/z* 572 and weak molecular ion peaks $[Zn_2L_2X(anion)]^+$ at *m/z* 1250 for **5** and 1028 for **6**.

The ^{1}H NMR spectrum of complex **5** can be assigned as follows; single sets of signals for the aromatic and methylene groups from L suggest that the pyridyl pendant arms in the two LZn units of the complex are equivalent in solution, even though the solid-state crystal structure shows small differences in bond lengths and angles for the pyridine co-ordination. Probably influenced by co-ordination to the zinc, the proton in the *ortho* position on the pyridyl group moves to δ 9.25 (doublet), as compared to δ 8.40 in the spectrum of free L. The ^{13}C NMR signals also correspond to the resonances of equivalent ligand arms, the bridging phosphate anion and the tetraphenylborate anion. The ^{31}P NMR peak at δ −0.6 is assigned to the co-ordinated phosphate group. The UV/VIS spectrum in MeOH solution exhibits two absorption bands at 258 (ε 29 600) and 304 nm (9300 dm^3 mol^{-1} cm^{-1}) in the region of 220–450 nm. On comparison with the spectrum of complex **7** the band at 304 nm can be assigned to the absorption of nitrophenolate group in the phosphate.

Treatment of complex **1** with Na_2HPO_4 in 90% methanol–water following the same reaction procedure as for **5** gave the crystalline solid product **7**. Elemental analysis suggests that is the dinuclear μ-phosphate complex [LZn{OP(O)(OH)O}ZnL][BPh_4]$_2$. The ^{31}P NMR signal at δ 2.21, assigned to HPO_4^{2-}, confirmed the presence of an inorganic phosphate. The IR absorptions of this phosphate group occur at 1269 and 1127 cm^{-1}. Only one absorption band at 258 nm (26 000 dm^3 mol^{-1} cm^{-1}), similar to the strong band of **4**, was found in the UV/VIS spectrum. The FAB mass spectrum exhibits dinuclear fragment peaks at *m/z* 1127 and 807, corresponding to the molecular ion and [$(ZnL)_2(HPO_4)$], respectively. The ^{1}H and ^{13}C NMR spectra also are consistent with the proposed formulation.

Complex **7**, which can be presumed to be similar in structure to that of **5** as it has very similar spectroscopic properties, it is interesting because it is more directly comparable with the dinuclear zinc site in the alkaline phosphatase–inorganic phosphate structure. Although some metal complexes[14,36–40] containing a bridging phosphate group are known, a dinuclear zinc complex bridged solely by an inorganic phosphate has not been reported; unfortunately suitable crystals of **7** have not yet been obtained for X-ray analysis.

Karlin and co-workers have described a series of copper(II) complexes of L which with further ligation from an exogenous neutral or anionic ligand can either form five-co-ordinated mononuclear[41,42] or X-bridged (X = F^-, O_2^{2-} or CO_3^{2-}) dinuclear[31,43,44] copper(II) species. The co-ordination properties of zinc(II) and copper(II) complexes of L stimulated interest in constructing a heterodinuclear metal (Zn–Cu) complex in the presence of a phosphate bridging group. The mononuclear complexes of both metals showed trigonal-bipyramidal co-ordination which was retained by zinc in the dication [LZn(*p*-$O_2NC_6H_4OPO_3$)Zn$L]^{2+}$ but not by copper in the dication [LCu(CO_3)LCu]$^{2+}$ in which a square-pyramidal geometry was noted and so it was hoped that retention of these environments would lead to site discrimination in a heterodinuclear complex. Complex **8** was synthesized as a crystalline product by following a similar procedure to that used to prepare **5**. Recrystallisation from MeOH–MeCN gave blue-green crystals.

Table 4 Selected bond lengths (Å) and angles (°) for [ZnCuL_2-(*p*-$O_2NC_6H_4OPO_3$)][BPh_4]$_2$·H_2O

Zn(1)–O(1)	1.858(8)				
Zn(1)–N(5)	2.048(9)	95.5(4)			
Zn(1)–N(6)	2.105(8)	173.8(4)	78.7(3)		
Zn(1)–N(7)	2.055(8)	105.5(4)	121.6(3)	79.6(3)	
Zn(1)–N(8)	2.046(7)	100.3(3)	115.8(3)	80.6(3)	113.0(3)
		O(1)	N(5)	N(6)	N(7)
Cu(1)–O(2)	1.903(7)				
Cu(1)–N(1)	2.093(8)	96.7(4)			
Cu(1)–N(2)	2.146(7)	177.4(3)	81.3(3)	79.8(3)	
Cu(1)–N(3)	1.989(9)	99.9(6)	122.6(3)	80.3(3)	
Cu(1)–N(4)	2.058(8)	102.0(4)	107.3(3)	N(2)	121.8(4)
		O(2)	N(1)		N(3)

The crystal structure of complex **8** shows that it consists of a heterodinuclear Zn–Cu^{II} dication, in which a phosphate group bridges the metals, two tetraphenylborate anions and a solvent water. Fig. 4 shows the molecular structure of the cation. The co-ordination environment at each metal is similar to those found in **5**. Each metal is five-co-ordinated by four N atoms from the ligand and one O atom from the bridging phosphate giving an approximately trigonal-bipyramidal geometry; no site discrimination was therefore detected. The three pyridyl N atoms are equatorially bonded to the metal; the bridgehead N atom from L and a phosphate O atom bind in axial positions with N–M–O angles of 177.4 and 173.8°. Each metal site was modelled at 50:50 disordered Cu:Zn. The metal atoms are displaced from the basal trigonal planes in the direction of the phosphate O atom by 0.153 and 0.154 Å respectively. The phosphate group has occupied the open axial positions created by tripodal ligation of the metal atoms and, on comparison with the phosphate in **5**, is significantly distorted with P–O–M angles of 158.9 and 155.2° respectively. Fig. 5 presents views of the dications in complexes **5** and **8** along the metal–metal axis and clearly shows the different conformations obtained.

Selected bond lengths and angles defining the co-ordination environment of the metal sites in complex **8** are listed in Table 4. The M–O bond distances are 1.858 and 1.903 Å and are the shortest bonds in each co-ordination sphere. The mean value of the metal–nitrogen bond lengths is 2.063 Å, in keeping with the distances found in the tripodal complexes discussed in this paper. On the basis of bond-angle data it can be shown that the two metal sites have closely trigonal-bipyramidal geometries (τ = 0.91 and 0.87); a perfect trigonal bipyramid has τ = 1 and a square pyramid τ = 0.[45] The Zn···Cu separation is 5.86 Å compared with the Zn···Zn separation of 5.97 Å in **5**. The solvent water is hydrogen bonded to the terminal phosphate oxygen O(3) *via* one O–H bond: it is not bridging. Thus the presence of this solvent prevents the disorder of the nitrophenyl sites found in the Zn_2 analogue.[26]

The IR spectrum of this complex is very similar to that of dinuclear zinc complex **5** with the P–O bands occurring at 1262 and 1128 cm^{-1}. The FAB mass spectrum reveals several fragment signals. The molecular ion peak is at *m/z* = 1246 (13%), and signals corresponding to di- and mono-nuclear fragments can be observed at *m/z* = 926 (37%) for [LZnXCuL] (X = phosphate), 572 (17%) for [ZnL(X)], 355 (46%) for [ZnL] and 353 (100%) for [CuL]. Further evidence for the formation of the heterodinuclear species was obtained from an accurate mass measurement for the fragment [LZn(X)CuL] which appears at

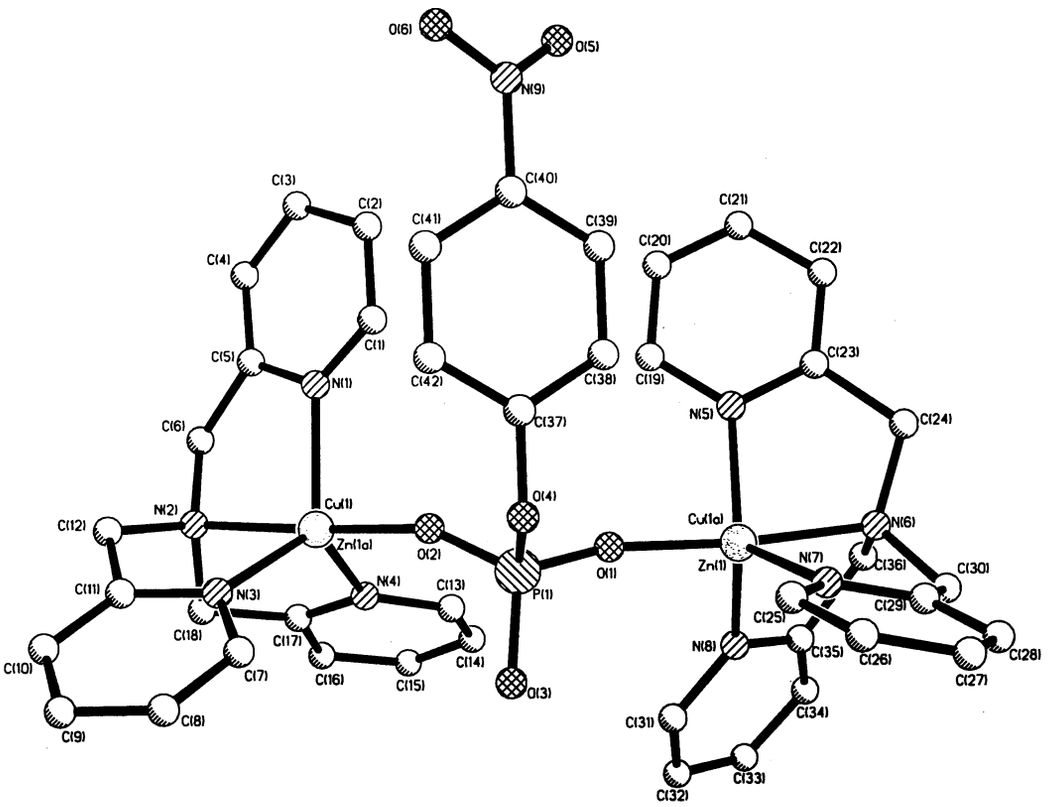

Fig. 4 Molecular structure of the dication $[LZn(p\text{-}O_2NC_6H_4OPO_3)CuL]^{2+}$

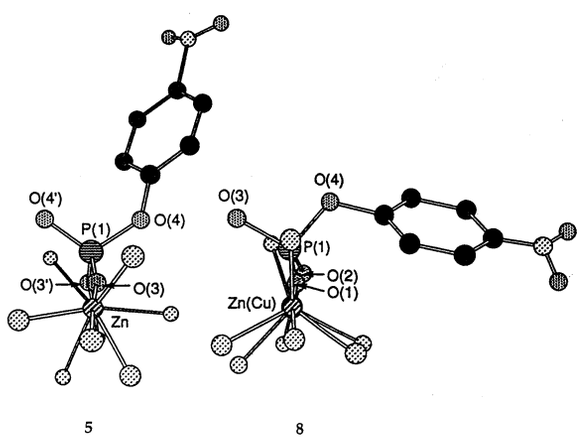

5 8

Fig. 5 Comparison of the metal co-ordination environments and the position of the phosphate group in complexes **5** and **8** viewed along the metal–metal axes

m/z = 924.142 021 as compared to the calculated value of 924.142 664; the isotopic pattern for this peak was fully consistent with the theoretical pattern.

As heteromultinuclear active sites have become more evident in metallo-proteins and -enzymes interest in the design and synthesis of co-ordination complexes capable of serving as small-molecule models for such sites has grown.[46] The successful synthesis and characterisation of the heterodinuclear (Cu–Zn) species herein is of interest because this is the first time that such a mixed zinc–copper complex bridged by a phosphate group has been prepared. Previously a limited number of imidazole-bridged heterodinuclear zinc–copper complexes having value as Cu–Zn bovine erythrocyte superoxide dismutase models has been reported.[47–51]

Acknowledgements

We thank the University of Sheffield for a Scholarship (to Q.-Y. H.) and EPSRC and the Royal Society for funds towards the purchase of the diffractometer. The data for the complex $[ZnCuL_2(p\text{-}O_2NC_6H_4OPO_3)][(BPh_4)]_2\cdot H_2O$ were recorded at Cardiff at the EPSRC facility.

References

1 E. E. Kim and H. W. Wyckoff, *J. Mol. Biol.*, 1991, **218**, 449
2 S. K. Burley, P. R. David, R. M. Sweet, A. Taylor and W. N. Lipscomb, *J. Mol. Biol.*, 1992, **224**, 113.
3 A. Volbeda, A. Lahm, F. Sakiyama and D. Suck, *EMBO J.*, 1991, **10**, 1607.
4 E. Hough, L. K. Hansen, B. Birknes, K. Jynge, S. Hansen, A. Hordvik, C. Little, E. Dodson and Z. Derewenda, *Nature* (*London*), 1989, **338**, 357.
5 M. M. Benning, J. M. Kuo, F. M. Raushel and H. M. Holden, *Biochemistry*, 1995, **34**, 7973.
6 B. Chevrier, C. Schalk, H. D'Orchymont, J. Rondeau, D. Moras and C. Tarnus, *Structure*, 1994, **2**, 283.
7 D. E. Fenton and H. Okawa, *J. Chem. Soc., Dalton Trans.*, 1993, 1349.
8 B. L. Vallee and D. S. Auld, *Biochemistry*, 1993, **32**, 6493.
9 N. Sträter, W. N. Lipscomb, T. N. Klabunde and B. Krebs, *Angew. Chem., Int. Ed. Engl.*, 1996, **35**, 2024.
10 W. N. Lipscomb and N. Sträter, *Chem. Rev.*, 1996, **96**, 2375.
11 D. E. Wilcox, *Chem. Rev.*, 1996, **96**, 2435.
12 N. N. Murthy and K. D. Karlin, *J. Chem. Soc., Chem. Commun.*, 1993, 1236.
13 R. G. Clewley, H. Slebocka-Tilk and R. S. Brown, *Inorg. Chim. Acta*, 1989, **157**, 233.
14 S. Hikichi, M. Tanaka, Y. Moro-oka and N. Kitajima, *J. Chem. Soc., Chem. Commun.*, 1992, 814.
15 S. Uhlenbrock and B. Krebs, *Angew. Chem., Int. Ed. Engl.*, 1992, **31**, 1647
16 P. Chaudhuri, C. Stockheim, K. Wieghardt, W. Deck, R. Gregorzik, H. Vahrenkamp, B. Nuber and J. Weiss, *Inorg. Chem.*, 1992, **31**, 1451.
17 M. Ruf, K. Weis and H. Vahrenkamp, *J. Am. Chem. Soc.*, 1996, **118**, 9288.
18 B. L. Vallee and D. S. Auld, *Proc. Natl. Acad. Sci. USA*, 1990, **87**, 220.
19 B. L. Vallee and D. S. Auld, *Biochemistry*, 1990, **29**, 5647.
20 J. Chin, *Acc. Chem. Res.*, 1991, **24**, 145.
21 J. Suh, *Acc. Chem. Res.*, 1992, **25**, 273.
22 E. Kimura, *Comments Inorg. Chem.*, 1991, **11**, 285.

23 D. W. Christiansen and W. N. Lipscomb, *Acc. Chem. Res*., 1989, **22**, 62.
24 D. N. Silverman and S. Lindskog, *Acc. Chem. Res*., 1988, **21**, 30.
25 G. Anderegg, E. Hubmann, N. G. Podder and F. Wenk, *Helv. Chim. Acta*, 1977, **60**, 123.
26 H. Adams, N. A. Bailey, D. E. Fenton and Q.-Y. He, *J. Chem. Soc.*, *Dalton Trans*, 1995, 697.
27 G. Anderegg and F. Wenk, *Helv. Chim. Acta*, 1967, **50**, 2330.
28 G. M. Sheldrick, SHELXL 93, An integrated system for solving and refining crystal structures from diffraction data, University of Göttingen, 1993.
29 C. S. Allen, C.-L. Chuang, M. Cornebise and J. W. Canary, *Inorg. Chim. Acta*, 1995, **239**, 29.
30 R. Gregorizik, U. Hartman and H. Vahrenkamp, *Chem. Ber.*, 1994, 2117.
31 Z. Tyeklar, P. P. Paul, R. R. Jacobson, A. Farooq, K. D. Karlin and J. Zubieta, *J. Am. Chem. Soc.*, 1989, **111**, 388.
32 R. Han, A. Looney, K. McNeill, G. Parkin, A. L. Rheingold and B. S. Haggerty, *J. Inorg. Biochem*., 1993, **49**, 105.
33 U. Hartman, R. Gregorizik and H. Vahrenkamp, *Chem. Ber.*, 1994, 2123.
34 Q.-Y. He, Ph.D. Thesis, University of Sheffield, 1995.
35 S. Hikichi, M. Tanaka, Y. Moro-oka and N. Kitajima, *J. Chem. Soc*., *Chem. Commun*., 1992, 814.
36 D. R. Jones, L. F. Lindoy, A. M. Sargeson and M. R. Snow, *Inorg. Chem*., 1982, **21**, 4155.
37 S. Drueke, K. Wieghardt, B. Nuber, J. Weiss, H. P. Fleischhauer, S. Gehring and W. Haase, *J. Am. Chem. Soc*., 1989, **111**, 8622.
38 P. N. Turowski, W. H. Armstrong, M. E. Roth and S. J. Lippard, *J. Am. Chem. Soc*., 1990, **112**, 681.
39 R. E. Norman, S. Yan, L. Que, jun., J. Sanders-Loehr, G. Backes, J. Ling, J. H. Zhang and C. J. O'Connor, *J. Am. Chem. Soc*., 1990, **112**, 1554.
40 J. E. Sarneski, M. Didiuk, H. H. Thorp, R. H. Crabtree, G. W. Brudvig, J. W. Faller and G. K. Schulte, *Inorg. Chem*., 1991, **30**, 2833.
41 K. D. Karlin, J. C. Hayes, S. Juen, J. P. Hutchinson and J. Zubieta, *Inorg. Chem*., 1982, **21**, 4106.
42 R. R. Jacobson, Z. Tyeklar, K. D. Karlin and J. Zubieta, *Inorg. Chem*., 1991, **30**, 2035.
43 R. R. Jacobson, Z. Tyeklar, A. Farooq, K. D. Karlin, S. Liu and J. Zubieta, *J. Am. Chem. Soc.*, 1988, **110**, 3690.
44 Z. Tyeklar, R. R. Jacobson, N. Wei, N. N. Murthy, J. Zubieta and K. D. Karlin, *J. Am. Chem. Soc*., 1993, **115**, 2677.
45 A. W. Addison, T. N. Rao, J. Reedijk, J. van Rijn and G. C. Vershoor, *J. Chem. Soc.*, *Dalton Trans.*, 1984, 1349.
46 D. E. Fenton and H. Okawa, *Chem. Ber./Recueil*, 1997, **130**, 433.
47 M. Sate, S. Nagae, M. Uehara and J. Nakaya, *J. Chem. Soc.*, *Chem. Commun*., 1984, 1661.
48 Q. Lu, Q. Luo, A. B. Dai and G. H. Hu, *J. Chem. Soc.*, *Chem. Commun*., 1990, 1429.
49 Z. W. Mao, K. B. Yu, D. Chen, S. Y. Han, Y. X. Sui and W. X. Tang, *Inorg. Chem*., 1993, **32**, 3104.
50 Z. W. Mao, D. Chen, W. X. Tang, K. B. Yu and L. Liu, *Polyhedron*, 1992, **11**, 191.
51 J.-L. Pierre, P. Chautemps, S. Refaif, C. Beguin, A. E. Marzouki, G. Serratrice, E. Saint-Aman and P. Rey, *J. Am. Chem. Soc*., 1995, **117**, 1965.

Received 16*th December* 1996; *Paper* 6/08406K